Tunable coupling of a hybrid plasmonic waveguide consisting of two identical dielectric cylinders and a silver film*

Benli Wang(王本立)[1,†], Han Liang(梁涵)[1], and Jiafang Li(李家方)[2]

[1] *Department of Physics, Beijing University of Chemical Technology, Beijing* 100029, *China*

[2] *Beijing National Laboratory for Condensed Matter Physics and Institute of Physics, Chinese Academy of Sciences, Beijing* 100190, *China*

(Received 21 February 2017; revised manuscript received 3 July 2017; published online 30 September 2017)

The propagation length of surface plasmon polaritons (SPPs) is intrinsically limited by the metallic ohmic loss that is enhanced by the strongly confined electromagnetic field. In this paper, we propose a new class of hybrid plasmonic waveguides (HPWs) that can support long-range SPP propagation while keeping subwavelength optical field confinement. It is shown that the coupling between the waveguides can be well tuned by simply varying the structural parameters. Compared with conventional HPWs, a larger propagation length as well as a better optical field confinement can be simultaneously realized. The proposed structure with better optical performance can be useful for future photonic device design and optical integration research.

Keywords: surface plasmon polaritons, hybrid plasmonic waveguide, optical field confinement

PACS: 41.20.Jb, 42.82.Et **DOI:** 10.1088/1674-1056/26/11/114103

1. Introduction

Surface plasmon polaritons (SPPs) have been widely investigated owing to their special characteristics[1–4] as well as potential applications in many areas such as plasmonic detectors and optical devices.[5–11] One fundamental property of SPPs is that they can induce strong optical field enhancement and confinement,[3,4] which makes them promising for the manipulation of light on the nanoscale.[12] Plasmonic optical devices, such as ultrafast optical switch,[13–15] plasmonic waveguide,[16–19] light coupler,[20,21] and nonlinear optical devices have been extensively studied.[22–25]

However, optical integration is one of the most important and interesting topics in nanophotonics.[26,27] In this aspect, plasmonic waveguides, based on the propagation of SPPs, have attracted great attention as an ideal candidate for optical integration.[16,17,28,29] However, the propagation length is shortened because of the intrinsic ohmic loss of metals. In order to obtain long-range propagation and good optical field confinement, a hybrid plasmonic waveguide (HPW) consisting of a semiconductor nanowire near a metal surface was introduced.[30] Other types of HPWs were studied as well,[31–33] with preferable tunability[34,35] and broadband coupling functionalities.[36] Researchers also investigated the optical force in a hybrid system theoretically.[37] These results showed that an HPW is a promising design for the studies on optical integration. In order to increase the propagation length of the hybrid mode with moderate field confinement, we further investigate the HPW here.

In this paper, we propose a new type of HPW that consist of two identical dielectric cylinders and a silver film, referred to as a coupled HPW (CHPW). The optical properties of cylindrical semiconductor nanowires can be controlled by using the metal cluster-catalyzed vapor–liquid–solid growth mechanism, and methods for the hierarchical assembly of nanowires into functional devices were also described.[38] A plasmonic nanolaser using an HPW was reported.[39] The method of making identical single crystalline microwires can be useful as well.[40] Compared with a conventional HPW that consists of a single dielectric waveguide and a silver film, our system introduces a new coupling factor of two cylinders, which induces more freedom regarding the tuning of the HPW. Our work demonstrates that this proposed CHPW not only can realize long-range propagation, but also can keep strong optical field confinement. It also shows better optical performance than conventional HPWs by comparison.

2. Theory

The coupled-mode theory is used to investigate the CHPW. If we consider one-order approximation, the hybrid mode can be written as[30]

$$\psi_{\pm}(D,r,h) = a_{\pm}(D,r,h)\psi_{\mathrm{cyl}}(r) + b_{\pm}(D,r,h)\psi_{\mathrm{spp}}, \qquad (1)$$

where ψ_{cyl} denotes the cylinder basis mode and ψ_{spp} is the SPP mode. $a_{\pm}(D,r,h)$ and $b_{\pm}(D,r,h)$ are the amplitudes of the cylinder mode and SPP mode, respectively. In this paper, D means the gap between two dielectric cylinders, r denotes the radius of the cylinder, and h is the distance between the

*Project supported by the National Natural Science Foundation of China (Grant No. 11647021) and the Fundamental Research Funds for the Central Universities of China (Grant No. ZY1531).

†Corresponding author. E-mail: wangbenli@mail.buct.edu.cn

© 2017 Chinese Physical Society and IOP Publishing Ltd

cylinders and a silver film. Here, the influence of the interaction between the two dielectric cylinders is added to the amplitude parameter because it is quite weak compared to that between the cylinder mode and the SPP mode. The cylinder basis mode and the SPP mode can be denote as $\{1\ 0\}^{\mathrm{T}}$ and $\{0\ 1\}^{\mathrm{T}}$, respectively.

Under one-order approximation, the amplitudes of the cylinder mode and SPP mode have the following relation

$$a_{\pm}(D,r,h)^2 + b_{\pm}(D,r,h)^2 = 1. \tag{2}$$

The modes of the system are characterized by the system of equations

$$\begin{bmatrix} n_{\mathrm{cyl}}(r) & C(r,h) \\ C(r,h) & n_{\mathrm{SPP}} \end{bmatrix} \begin{bmatrix} a_{\pm}(D,r,h) \\ b_{\pm}(D,r,h) \end{bmatrix} = n_{\pm}(D,r,h) \begin{bmatrix} a_{\pm}(D,r,h) \\ b_{\pm}(D,r,h) \end{bmatrix}. \tag{3}$$

Here, $n_{\mathrm{cyl}}(r)$ is the effective index of the cylinder basis mode, n_{SPP} is the effective index of the SPP mode, and $n_{\pm}(D,r,h)$ are the effective indices of the hybrid modes. $C(r,h)$ means the coupling strength of the cylinder basis mode and SPP mode.

By combining Eqs. (2) and (3), we can get

$$a_{\pm}^2 = \frac{n_{\pm} - n_{\mathrm{SPP}}}{(n_{\pm} - n_{\mathrm{SPP}}) + (n_{\pm} - n_{\mathrm{cyl}})}, \tag{4}$$

$$C = \sqrt{(n_{\pm} - n_{\mathrm{cyl}})(n_{\pm} - n_{\mathrm{SPP}})}. \tag{5}$$

Then, the coupling between the cylinder mode and the SPP mode can be analyzed by the above-derived equations. The 2D-finite-difference numerical method is used in our calculations,[32] and the optical modes are solved in the cross-section of the CHPW. The configuration of the CHPW is shown in Fig. 1. The yellow part denotes the silver film. The red nanowires are the identical high-index dielectric waveguides, and the green part means the surrounding low-index dielectric material. The permittivity of the low-index dielectric material is 2.25, and it is 12.25 for the high-index dielectric waveguide. The communication wavelength $\lambda = 1.55$ μm is considered here. The permittivity of silver is described as[41]

$$\varepsilon = -129 + 3.3\mathrm{i}. \tag{6}$$

First, the effective index of the SPP mode on the interface of the silver film and dielectric materials can be calculated theoretically. The SPP mode is excited when the wave vector of the propagation constant of the evanescent wave from the dielectric cylinder matches that of the surface plasmon. Then the effective indices of the cylinder mode and hybrid mode can be obtained by numerical calculations. Finally, the coupling strength and the amplitude of the basis mode can be obtained by the coupled-mode theory described above. There exists a symmetric mode and an anti-symmetric mode for both two identical dielectric cylinders' structure and CHPW structure. However, when the radius of the dielectric cylinder is small, e.g., 100 nm, the lower index mode ("anti-symmetric") is cut-off and the hybrid mode with lower index cannot exist. Besides, the propagation length of the anti-symmetric mode is shorter than that of the symmetric mode. Therefore, we are interested only in the symmetric mode in this work.

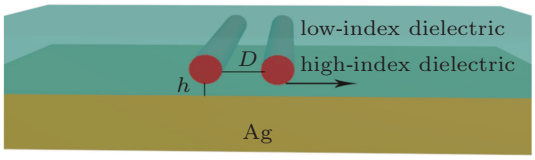


Fig. 1. (color online) Configuration of the HPW. The yellow part denotes the silver film. The red cylinders are high-index waveguides, and the refractive index is 3.5. The green part means the low-index dielectric material, and the refractive index is 1.5.

3. Results and discussion

The effective index of CHPWs as a function of the radius of cylinders for different h is presented in Fig. 2(a). Here, the gap between the two cylinders is fixed at 10 nm. The black solid curve is the effective index of the cylinder mode as a function of the radius of the cylinders. Other colorful solid curves denote the effective indices of the CHPWs for different h. It can be seen that as the radius of the cylinders enlarge gradually, the hybrid effective index increases monotonically. It is because the effect of the dielectric cylinder mode on the hybrid mode increases with the radius of thecylinders. We can also find that as the distance between the silver film and the cylinders decreases, the hybrid effective index increases due to coupling enhancing.

To further understand the coupling effect, the propagation length is also calculated, and the results are shown in Fig. 2(b). The red and black dotted lines mean the propagation lengths of the pure SPP modes at the silver-low-index dielectric material and silver-high-index dielectric material interfaces,respectively, and the values are 359.23 μm and 25.003 μm. The colored curves denote the propagation lengths of the hybrid modes in the CHPWs with different h. We can find that the propagation lengths of the hybrid modes show nonmonotonic trend, but increase monotonically with the radius of the cylinders when the radius is larger than a certain value of around 100 nm. It can be seen that in some cases the propagation lengths of the hybrid modes can surpass that of the pure SPP mode at the silver-low-index dielectric material interface. It means that the attenuation can be reduced by this kind of CHPWs and the propagation length can be extended. From Fig. 2(b), we can see that the uttermost increment of the propagation length reaches about two orders comparing to that of the pure SPP mode at the silver-low-index dielectric material interface.

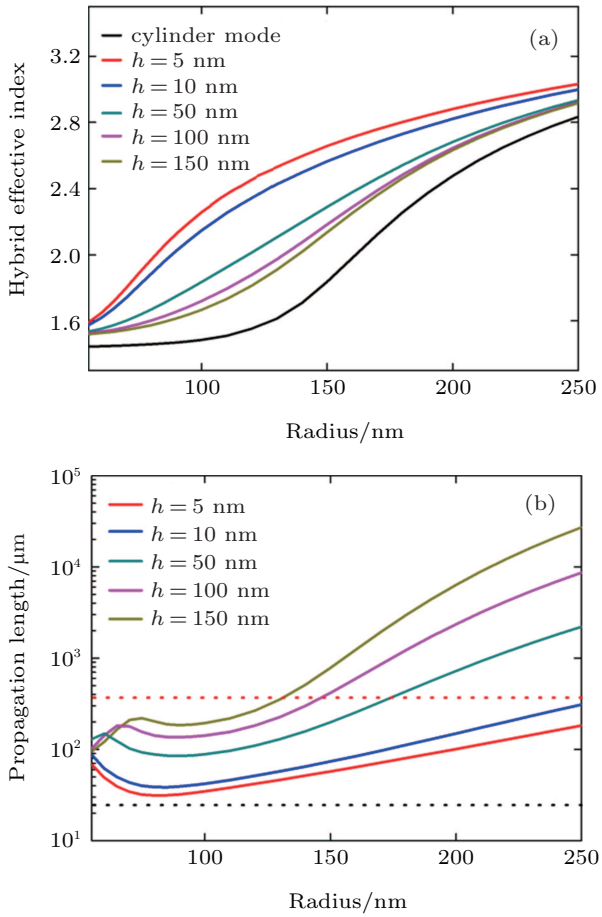


Fig. 2. (color online) (a) Hybrid effective index varies with the radius of the cylinders for different HPWs. (b) The propagation length as a function of the radius of the cylinders for different HPWs. The black line denotes the hybrid effective index of the cylinder mode, and other colored lines mean the hybrid effective index of the hybrid mode in CHPWs with different h.

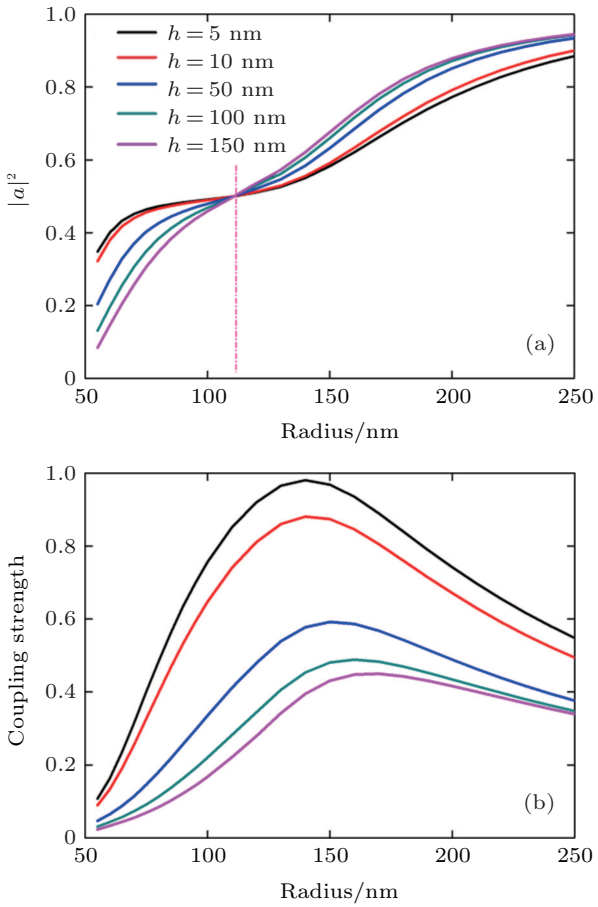


Fig. 3. (color online) (a) Expansion coefficient of the cylinder mode. (b)The coupling strength of the cylinder mode and SPP mode. The gap between the two cylinders is fixed at 10 nm. The legend of (b) is the same as that of (a).

In order to understand the underlying physics behind the CHPW, we also calculated the amplitude of the cylinder mode and the coupling strength based on Eqs. (4) and (5). The square of the amplitude of the cylinder mode is shown in Fig. 3(a). The dotted vertical line denotes the point of intersection of all the curves, and the square of the amplitude of the cylinder mode is equal to 0.5 at that position where the radius of the cylinders is approximately 110 nm. It means that below the position, the hybrid mode demonstrates an SPP-like characteristic, and above that position, the hybrid mode shows a cylinder-like characteristic. That also illustrates the characteristics of the propagation lengths in Fig. 2(b). The coupling strength is presented in Fig. 3(b). It can be found that the coupling strength is similar to parabola and has a maximum for all the CHPWs with different h. It is evident that the coupling effect is stronger for smaller h. If h is fixed, the coupling strength first increases and then decreases with the increase of the radius of the cylinders. By varying the parameters of the CHPWs, the peak of the coupling strength can also be tuned.

The modal field distributions are also calculated in order to make clear the physical picture of the CHPW. The modal field intensity distributions are shown in Figs. 4(a)–4(e), where (a)–(e) denote the CHPWs with different h. The gap between the cylinders is 10 nm, and the radius of the cylinders is fixed at 125 nm. All the electric fields are normalized. It can be easily found that the modal field intensities are mainly confined in the gap between the cylinders and the silver film, especially for those with h below 50 nm. In order to evaluate the field confinement quantitatively, the field intensities are integrated over different surfaces. We find if the integration surface is defined by the gap area between the cylinders and the silver film, the fraction integrated is about 50%, and if the cylinder area is added to the integration surface, the fraction integrated will account for about 90%. Therefore, it is reasonable to consider this area to describe the field confinement. By performing a simple calculation, we find that the area is about 0.2 μm^2 for the HPW with $h = 150$ nm. It is about two times smaller than the diffraction-limited area in free space ($\lambda^2/4$).[34] It means that strong field confinement can be achieved while long-range propagation is obtained.

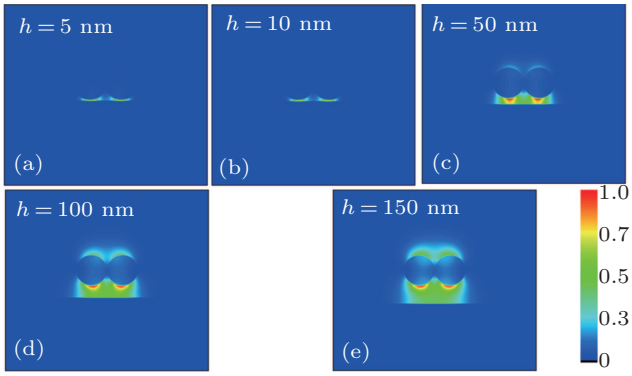


Fig. 4. (color online) Modal field intensity distribution with (a) $h = 5$ nm, (b) $h = 10$ nm, (c) $h = 50$ nm, (d) $h = 100$ nm, and (e) $h = 150$ nm.

In order to obtain a direct picture of the optical performance of the CHPW, we make a detailed comparison between its field confinement and that of a conventional HPW.[30] Here, the field confinement is described by the area, in which the proportion of the mode energy that propagates is about 90%. The conventional definition of the modal area is not adopted because it cannot reflect the field confinement well. We can find that the proportion is about 25% for a conventional HPW with $h = 2$ nm.[30] The modal areas described above are both calculated for the new HPW and the conventional HPW. The results are shown in Fig. 5. The gap between the dielectric cylinders is fixed at 10 nm for the CHPWs. The modal areas for both HPWs with different h are calculated. The black line denotes the modal area for the conventional HPW, and the red one is for the CHPW. We can find that the areas for the CHPW are always much smaller than that for the conventional HPW. When h is equal to 150 nm, the area for the conventional HPW is almost two times bigger than that for the CHPW. This illustrates that the new proposed CHPW has much better field confinement than the conventional HPW. Besides, because of the existence of the coupling effect between nanowires, it can be expected that the CHPW will show better field confinement than a similar HPW proposed in Ref. [31] by making a simple comparison of the modal field distributions.

The effect of the coupling between the cylinders on the hybrid modes is also discussed here. The gap between the cylinders is changed to 20 nm and 50 nm. Here, the propagation lengths of the hybrid modes in the CHPWs with $h =$ 50 nm, 100 nm, and 150 nm are presented in Fig. 6. The inset of Fig. 6 is the part of the propagation length of the hybrid mode in the HPW with $h = 50$ nm. The inset shows that in a small-size area (e.g., $r < 100$ nm) the propagation length increases with the enlargement of the gap (d), while in a large-size area (e.g., $r > 180$ nm) it decreases with the enlargement of the gap. Based on the previous discussion, it can be concluded that a small gap is more advantageous for modal field confinement than a large gap. This indicates that by tuning the gaps of the CHPWs, we can realize a higher quality CHPW with long-range propagation while reducing the modal field area.

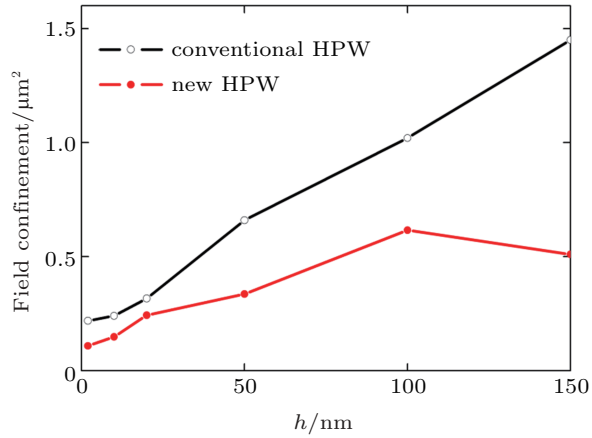


Fig. 5. (color online) Field confinement as a function of the distance (h) between the silver film and the dielectric cylinders. Here, the field confinement strength is described by the area, in which the proportion of the mode energy that propagates is about 90%. The red line means that for our proposed HPW, and the black one is for the conventional HPW.

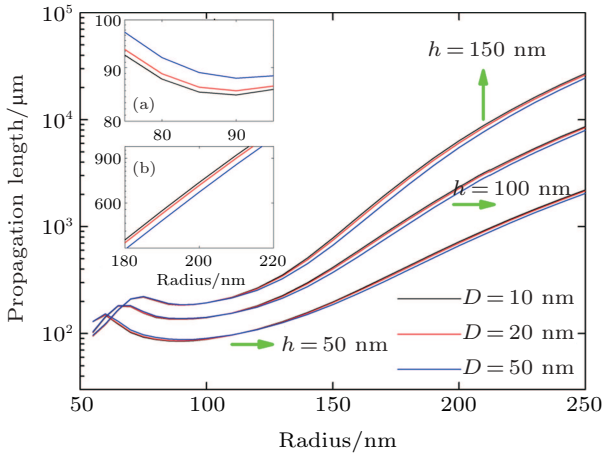


Fig. 6. (color online) Propagation length varies with the radius of the cylinders for different HPWs with different gaps (D) of the cylinders and distances between the silver film and the cylinders (h). The inset shows the part of the propagation length of the HPW with $h = 50$ nm.

The changes in the refractive index of semiconductor nanowires can be from 0.01 to 0.1 by injection of free carriers and multiple quantum wells.[42] The optical properties of the CHPWs are estimated to be adjusted by this method. Therefore, the effect of the refractive index of cylindrical nanowires on the coupling is considered. The changes in the refractive index of the cylindrical waveguides are set to 0.02 and 0.1. The gap of the cylindrical waveguides is fixed at 10 nm, and the distance between the cylindrical waveguides and the silver film is 50 nm. The results are shown in Figs. 7(a)–7(d), where figure 7(a) is the hybrid effective index, figure 7(b) is the propagation length, figure 7(c) is the expansion coefficient of the cylinder mode, and figure 7(d) is the coupling strength. Figure 7(a) shows that as the radius of the cylinders increases, the difference of the hybrid effect index induced by the variance

of the refractive index becomes larger, and we can find that the maximum difference of the hybrid effect index can reach approximately 0.2. The propagation length shown in Fig. 7(b) first decreases as the refractive index of the cylinders increases when the radius of the cylinders is below than 120 nm, but then it changes similarly to the refractive index of the cylinders. The maximum increase in the propagation length is approximately 848 μm, which is much larger than that of the pure SPP mode at the silver-low-index dielectric material interface. We can also find that the coupling strength is easily tuned by changing the refractive index of the cylinders for the hybrid mode with the SPP-like characteristic, but the expansion coefficient of the cylinder mode can be adjusted by varying the refractive index of the cylinders for the hybrid mode with the cylinder-like characteristic from Figs. 7(d) and 7(c). Thus, we can conclude that the optical properties of the hybrid mode in the proposed CHPW can be tuned by varying the refractive index of the cylinders. This means that we can still tune the hybrid mode in the CHPW even when the structure parameters are fixed.

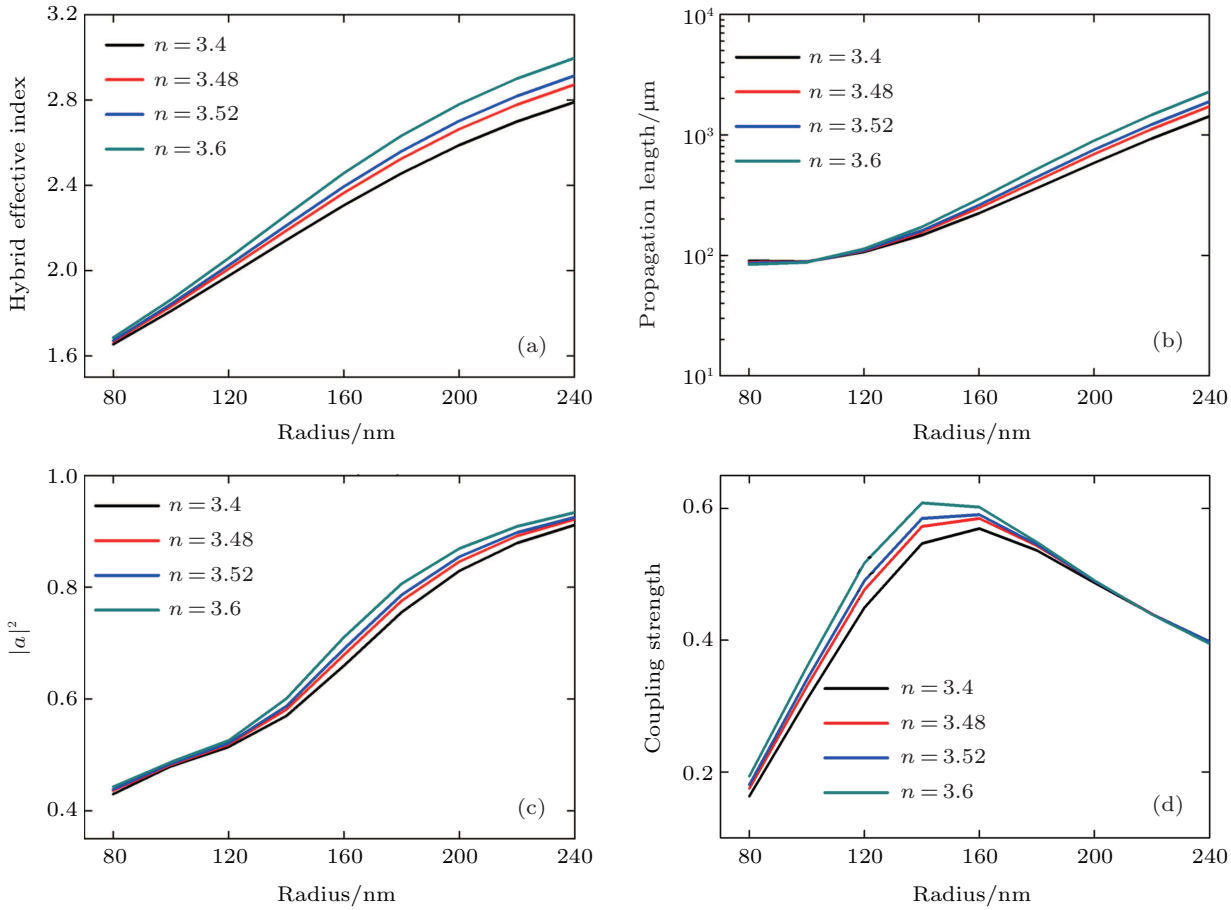


Fig. 7. (color online) (a) Hybrid effective index as a function of the cylinder radius with different refractive indices n. (b) Propagation length. (c) Expansion coefficient of the cylinder mode. (d) Coupling strengths of the cylinder mode and SPP mode. The changes in the refractive indices are 0.1 and 0.02, and the initial refractive index of the cylinders is 3.5. The refractive index n has four different values, which are 3.4, 3.48, 3.52, and 3.6.

4. Conclusions

In summary, a new class of HPWs is introduced, in which long-range propagation can be achieved while the subwavelength mode size is kept. By tuning the parameters of the HPW, the mode features can be adjusted. Comparisons with previous works show that the HPW proposed in this paper not only can hold better optical performance, but also can provide more flexibility in tunability. We also analyzed the dependence of the coupling on the changes in the refractive index of the cylindrical waveguides. Our configuration is expected to be more practical in applications compared with similar HPWs proposed. Our work could be useful for the design of HPWs and other optical devices as well as beneficial to integrated optics.

References

[1] Stern E A and Ferrell R A 1960 *Phys. Rev.* **120** 130
[2] Sarid D 1981 *Phys. Rev. Lett.* **47** 1927
[3] Barnes W L, Dereux A and Ebbesen T W 2003 *Nature* **424** 824
[4] Schuller J A, Barnard E S, Cai W, Jun Y C, White J S and Brongersma M L 2010 *Nat. Mater.* **9** 193
[5] Slavik R and Homola J 2006 *Opt. Commun.* **259** 507
[6] Rajan A, Sharma K and Gupta B D 2007 *J. Opt. A: Pure Appl. Opt.* **9** 682
[7] Homola J 2008 *Chem. Rev.* **108** 462

[8] Dyer G C, Vinh N Q, Allen S J, Aizin G R, Mikalopas J, Reno J L and Shaner E A 2010 *Appl. Phys. Lett.* **97** 193507

[9] Falk A L, Koppens F H L, Yu C L, Kang K, Snapp N D L, Akimov A V, Jo M H, Lukin M D and Park H 2009 *Nat. Phys.* **5** 475

[10] Zijlstra P, Paulo P M R and Orrit M 2012 *Nat. Nanotechnology* **7** 379

[11] Wang B L, Li J F and Li Z Y 2013 *J. Opt. Soc. Am. B* **30** 1590

[12] Ozbay E 2006 *Science* **311** 189

[13] Nikolajsen T, Leosson K and Bozhevolnyi S I 2004 *Appl. Phys. Lett.* **85** 5833

[14] Dintinger J, Klein S and Ebbesen T W 2006 *Adv. Mater.* **18** 1267

[15] MacDonald K F, Sámson Z L, Stockman M I and Zheludev N I 2009 *Nat. Photonics* **3** 55

[16] Gramotnev D K and Pile D F P 2004 *Appl. Phys. Lett.* **85** 6323

[17] Verhagen E, Kuipers L and Polman A 2007 *Nano Lett.* **7** 334

[18] Xue W R, Guo Y N and Zhang W M 2010 *Chin. Phys. B* **19** 017302

[19] Zhang H X, Gu Y and Gong Q H 2008 *Chin. Phys. B* **17** 2567

[20] Lou F, Wang Z, Dai D, Thylen L and Wosinski L 2012 *Appl. Phys. Lett.* **100** 241105

[21] Bozhevolnyi S I and Volkov V S 2004 *Phil. Truns. R. Soc. Lond. A* **362** 757

[22] Pu Y, Grange R, Hsieh C L and Psaltis D 2010 *Phys. Rev. Lett.* **104** 207402

[23] Kauranen M and Zayats A V 2012 *Nat. Photonics* **6** 737

[24] Nieuwstadt J A H V, Sandtke M, Harmsen R H, Segerink F B, Prangsma J C, Enoch S and Kuipers L 2006 *Phys. Rev. Lett.* **97** 146102

[25] Wang B L, Wang R, Liu R J, Lu X H, Zhao J and Li Z Y 2013 *Sci. Rep.* **3** 2358

[26] Almeida V R, Barrios C A, Panepucci R R and Lipson M 2004 *Nature* **431** 1081

[27] Li Z Y 2015 *Europhys. Lett.* **110** 14001

[28] Stockman M I 2004 *Phys. Rev. Lett.* **93** 137404

[29] Srivastava T, Das R and Jha R 2010 *Appl. Phys. Lett.* **97** 213104

[30] Oulton R F, Sorger V J, Genov D A, Pile D F P and Zhang X 2008 *Nat. Photonics* **2** 496

[31] Dai D and He S 2009 *Opt. Express* **17** 16646

[32] Zhao Y and Zhu L 2010 *J. Opt. Soc. Am. B* **27** 1260

[33] Chen L, Zhang T, Li X and Huang W P 2012 *Opt. Express* **20** 20535

[34] Bian Y S and Gong Q H 2014 *Sci. Rep.* **4** 6617

[35] Jiang M M, Chen H Y, Shan C X and Shen D Z 2014 *Phys. Chem. Chem. Phys.* **16** 16233

[36] Song Y, Wang J, Li Q, Yan M and Qiu M 2010 *Opt. Express* **18** 13173

[37] Yang X D, Liu Y M, Oulton R F, Yin X B and Zhang X 2011 *Nano Lett.* **11** 321

[38] Huang Y and Lieber C M 2004 *Pure Appl. Chem.* **76** 2051

[39] Oulton R F, Sorger V J, Zentgraf T, Ma R M, Gladden C, Dai L, Bartal G and Zhang X 2009 *Nature* **461** 629

[40] Wang K Y, Sun W Z, Wang S, Liu S, Zhang N, Xiao S M and Song Q H 2017 *Adv. Optical Mater.* **5** 1600744

[41] Zhu Z and Brown T G 2002 *Opt. Express* **10** 853

[42] Bennett B R, Soref R A and Alamo J A D 1990 *IEEE J. Quantum Electronics* **26** 113